

An Algorithm to Predict the Biomechanical Stiffening Effect in Corneal Cross-linking

Sabine Kling, PhD; Farhad Hafezi, MD, PhD

ABSTRACT

PURPOSE: To develop an algorithm to predict the stiffening effect of CXL and to verify the accuracy with results obtained from experimental measurements.

METHODS: The algorithm considers different variables: the reaction kinetics of riboflavin diffusion and riboflavin photodegradation to determine the effective riboflavin concentration in different stromal layers; the oxygen diffusion and ultraviolet (UV) absorption to determine the amount of reactive oxygen species as a function of time and stromal depth. For the experimental comparison, corneas were deepithelialized, followed by riboflavin instillation for 30 minutes and UV irradiation. Different pulsed and continuous-light conditions were analyzed with irradiances ranging from 3 to 100 mW/cm² and irradiation times from 8 to 30 minutes. Stress-relaxation measurements were performed in fresh-enucleated porcine (n = 66) and rabbit (n = 2) eyes directly after treatment, using a load of 0.6 MPa.

RESULTS: A clear linear relationship was observed between the concentration of newly induced cross-links and the experimentally observed stiffening factor ($R^2 = 0.9432$). An additional 1 mol/m³ of cross-links increased the mechanical stress resistance of the cornea by 50.4%. The efficacy of standard CXL in murine, lapine, and porcine corneas was inversely related to corneal thickness. The stiffening effect after CXL decreased by 4.1% per 100 μm ($R^2 = 0.9961$).

CONCLUSIONS: The proposed model, supported by data in porcine, murine, and lapine corneas, suggests a possibility of also predicting the biomechanical CXL efficacy in human corneas. The biomechanical efficacy of CXL may be increased by prolonged UV irradiation at reduced irradiances or by a higher oxygen pressure in the environment. Pulsed CXL does not accelerate CXL or increase its efficacy when compared to standard CXL of the same irradiation duration. This model might be used to calculate customized irradiation settings for high-risk cases, but also topography-guided CXL treatments.

[*J Refract Surg.* 2017;33(2):128-136.]

Corneal cross-linking (CXL) has the potential to become the standard treatment to arrest keratoconus progression. It is based on saturation of the corneal stroma with a photosensitizer and activating it with ultraviolet-A (UV-A) irradiation, which generates additional cross-links that increase the biomechanical resistance of the stroma.¹ Although CXL is being applied successfully in clinics with a failure rate of approximately 7.6% and a complication rate of 2.9%,² efforts are being made to increase CXL efficacy to shorten treatment time (lower costs) and improve patient comfort (less pain). Modified treatment protocols use different approaches: increasing UV irradiance to reduce irradiation time,³ applying riboflavin transepithelially to reduce postoperative pain and risk of infection,⁴ using iontophoresis to accelerate riboflavin diffusion and reduce soaking time,⁵ and using pulsed UV light to increase oxygen availability.⁶

Considering the current knowledge about CXL, all modifications have been promising. However, clinical practice proved transepithelial CXL being not,⁷ or less,⁴ effective and pulsed UV irradiation equivalent to continuous irradiation.⁸ Experimental studies showed a significantly decreased stiffening effect when using high irradiances.⁹⁻¹¹ The reason why these treatment protocols did not show the desired effect is because the mechanisms behind CXL and the interaction of different factors, such as UV energy, irradiation time, riboflavin diffusion capability, and oxygen availability, and reaction kinetics of CXL are poorly understood.

Although the stiffening effect after CXL has been extensively studied,^{9,11-17} so far only a few experimental studies have ad-

From the Center for Applied Biotechnology and Molecular Medicine, University of Zurich, Zurich, Switzerland (SK, FH); the Laboratory for Ocular Cell Biology, University of Geneva, Geneva, Switzerland (SK, FH); the Department of Ophthalmology, University of Southern California, Los Angeles, California (FH); and ELZA Institute, Dietikon/Zurich, Switzerland (FH).

Submitted: March 24, 2016; Accepted: November 10, 2016

The authors have no financial or proprietary interest in the materials presented herein.

Correspondence: Sabine Kling, PhD, Center for Applied Biotechnology and Molecular Medicine (CABMM), University of Zurich, Winterthurerstrasse 190, 8057 Zurich, Switzerland. E-mail: kling.sabine@gmail.com

doi:10.3928/1081597X-20161206-01

dressed the theoretical modeling of CXL. Schumacher et al.¹⁸ calculated the UV intensity and riboflavin concentration as a function of corneal depth and assumed that the product of both factors is proportional to the polymerization rate of the newly formed cross-links. Another, more precise model based on radical-initiated polymerization was proposed by Semchishen et al.¹⁹ These authors assumed a radical-initiated photopolymerization process, where each radical would become the center of a new polymer chain. However, the fast oxygen consumption²⁰ and the strong dependency on environmental oxygen²¹ in an experimental CXL setup make it likely that singlet oxygen is responsible for the formation of additional cross-links instead.

The clinical efficacy of CXL is analyzed in terms of the potential to stop keratoconus progression, or by the depth of the postoperative demarcation line observed in OCT images.^{22,23} The demarcation line has been considered to be an indicator of how deep CXL is effective²⁴ because additional cross-links are supposed to increase the density, which in turn changes the refractive index. Alternatively, the demarcation line could indicate the region of initial keratocyte apoptosis.

This study aimed to develop a theoretical model to predict the stiffening effect of CXL under different conditions, considering UV energy, light absorption, riboflavin and oxygen diffusion, available locations for cross-link formation, and rate constants, as a function of time and stromal depth. Furthermore, the objective of this study was to measure the experimental mechanical effect of different CXL protocols to verify the accuracy of the theoretical model.

MATERIALS AND METHODS

This study consists of an experimental and a theoretical part, which are compared to each other to verify the accuracy of the theoretical model.

THEORETICAL MODEL

On UV irradiation, the long-lived triplet state of riboflavin (approximately 1 ms) reacts with triplet oxygen to form singlet oxygen,²⁷ with the substrate to form riboflavin radicals, or with a quencher. Although both reaction products (singlet oxygen and riboflavin radicals) have the potential to induce cross-links, the oxygen content determines whether type I or II photochemical mechanisms dominate and how many cross-links can be induced. The type I mechanism involves the generation of radicals and consumes less oxygen than type II mechanism, which involves the generation of singlet oxygen.

Therefore, for the theoretical description of CXL we considered the following parameters: riboflavin concentration (diffusion/degradation), UV intensity, and

oxygen availability. Equations were formulated according to the biochemical reaction scheme shown in **Figure A** (available in the online version of this article). All equations were discretized and solved in customized programs written in Matlab (MathWorks, Bern, Switzerland) with a time step of 1/10 sec or smaller. The error due to step-size was less than 0.41%.

The first order rate constant for the uptake of oxygen and riboflavin from the corneal surface was estimated with Fick’s second law of diffusion. The integration of Fick’s law was approximated by twice applying the finite difference operator and by assuming that the concentration gradient within the cornea is negligible compared to the concentration gradient between environment and cornea. This leads to the following equation:

$$k[A] = \frac{\partial [A]}{\partial t} = D \cdot \frac{\partial^2 [A]}{\partial x^2} = D \cdot \frac{[A_{x+h}] - 2 \cdot [A_x] + [A_{x-h}]}{h^2} = D \cdot \frac{[A_0] - [A_{th}]}{(\Delta th)^2}$$

(eq. 1)

where $[A]$ represents the concentration of the diffusion medium, $k[A]$ the corresponding diffusion rate, th the stromal depth, $[A_0]$ the concentration on top of the corneal surface, and $[A_{th}]$ the concentration at a given stromal depth.

To describe the individual concentrations as a function of time and one dimension in space (ie, stromal depth), we used the integrated forms of first and second order rate equations for independent and competitive²⁸ reactions. The values of the constants used throughout the manuscript are listed in **Table A** (available in the online version of this article).

Accordingly, the riboflavin concentration in the cornea $[CO_{ribo}]$ is determined by the amount of uptake by diffusion and degradation by photolysis:

$$[CO_{ribo}] = [CO_{ribo}]_0 + \{t < t_{soak} \mid th_{riboTop} > 0\} \cdot [C_{ribo}] \cdot \left[1 - e^{-\frac{\Delta_{ribo}}{h^2} \cdot D_{ribo} \cdot \Delta th}\right] - \{[Photon] > 0\} \cdot [CO_{ribo}] \cdot (1 - e^{-k_{degRibo} \cdot \Delta t})$$

(eq. 2)

where Δ_{ribo} is the difference in riboflavin concentration between cornea and riboflavin solution, Δ_{ribo} is the diffusion coefficient of riboflavin, $k_{degRibo}$ is the first order rate constant of riboflavin degradation during UV irradiation, t is time, t_{soak} is soaking time with riboflavin, and t_{UV} is irradiation time. The $th_{riboTop}$ represents the thickness of the riboflavin layer on top of the corneal surface during irradiation and $[Photon]$ the photon concentration (see equation 6) resulting from the UV irradiation. The expressions within curly brackets represent if-statements.

The oxygen concentration in the cornea $[CO_{oxy}]$ is determined by the amount of uptake by diffusion, the cellular oxygen consumption of the stroma Q_{cell} , the

production and degradation of singlet oxygen and the oxidation of the reduced form of riboflavin:

$$[CO_{oxy}] = [CO_{oxy}]_0 + CO_{oxyhomeostatic} \cdot \left[1 - e^{-\frac{\Delta_{oxy}}{th^2} D_{oxy} t}\right] + [S_{oxy}] \cdot (e^{-k_{degSoxy} \Delta t} - 1) - [RFH_2] \cdot \left[1 - e^{-\frac{k_{qRibo}}{k_{RFH_{ox}}}[CO_{oxy}](1 - e^{-k_{RFH_{ox}} \Delta t})}\right] - \frac{Q_{cell}}{22.4L} \cdot \frac{Oxy_{tension}}{160mmHg} \cdot \Delta t$$

(eq. 3)

where Δ_{oxy} is the difference in oxygen concentration between the current and the normal oxygen content in the cornea, $[S_{oxy}]$ is the concentration of singlet oxygen, $k_{degSoxy}$ is the first order degeneration rate constant of singlet oxygen, $[RFH_2]$ is the concentration of the reduced form of riboflavin, k_{qRibo} is the quenching rate of riboflavin, $k_{RFH_{ox}}$ is the oxidation rate of the reduced form of riboflavin, Q_{cell} is the stromal oxygen consumption for a given oxygen tension $Oxy_{tension}$ ²⁹. The oxygen tension can be calculated from the oxygen concentration $[CO_{oxy}]$, the molar mass of oxygen and experimental data^{20,30}:

$$Oxy_{tension} = [CO_{oxy}] \cdot M_{O_2} \cdot \frac{102mmHg}{7.3 \frac{mg}{L}} \quad (\text{eq. 4})$$

$[EM]$ is the concentration of the estimated ratio of extracellular matrix (ie, collagen and non-collagenous proteins).

$$[EM] = \frac{0.18 \cdot \rho_{cornea}}{M_{collagen} \cdot N_A} - 400 \cdot [S_{oxy}] \cdot \left[1 - e^{-\frac{k_{RFH_{ox}}}{k_{EMox}}[EM] \cdot (1 - e^{-k_{EMox} \Delta t})}\right]$$

(eq. 5)

where $M_{collagen}$ is the molecular mass of collagen with approximately 407 Da ($6.76 \cdot 10^{-25}$ kg), ρ_{cornea} is the density of the cornea, and 0.18 is the assumed content of collagen and non-collagenous proteins in the cornea. Factor 400 is the authors' estimate to describe the reduction of possible additional cross-links per formed cross-link due to obstructing potential binding sites.

The concentration of photons in the cornea $[Photon]$ is determined by the absorbed UV energy along the cornea:

$$[Photon] = \frac{I_0 \cdot \Delta t \cdot \lambda \cdot (1 - 10^{-\alpha \cdot th - \epsilon \cdot [CO_{ribo}] \cdot (th + th_{riboTop})})}{h \cdot c \cdot N_A \cdot th} \quad (\text{eq. 6})$$

where I_0 is the nominal intensity of the UV lamp, λ is the wavelength, α is the absorption coefficient of the cornea stroma, ϵ is the extinction coefficient of riboflavin, th is the corneal thickness, $th_{riboTop} = 50 \mu m$ is the thickness of the riboflavin film³¹ on top of the cornea in the clinical setting, h is the Planck constant, c is the speed of light, and N_A is the Avogadro number.

The concentration of singlet oxygen is determined by the quantum yield of riboflavin, the singlet oxygen degradation through physical and chemical quenching, and the consumption of singlet oxygen during substrate oxidation:

$$[S_{oxy}] = [S_{oxy}]_0 + [CO_{oxy}] \cdot \left[1 - e^{-\Phi_{S_{oxy}} \frac{\epsilon [CO_{ribo}] th}{\epsilon [CO_{ribo}] (th + th_{riboTop}) + \alpha th} [Photon] (1 - e^{-k_{qRibo} \Delta t})}\right] - [S_{oxy}] \cdot \left[1 - e^{-\frac{k_{RFH_{ox}}}{k_{EMox}}[EM] \cdot (1 - e^{-k_{EMox} \Delta t})}\right]$$

(eq. 7)

where $\Phi_{S_{oxy}}$ is the quantum yield²⁶ of singlet oxygen production for riboflavin and k_{EMox} is the oxidation rate of the extracellular matrix.

The concentration of the riboflavin radical $[RFH^*]$ is given by:

$$[RFH^*] = [RFH^*]_0 + [EM] \cdot \left[1 - e^{-\Phi_{ISC} - \Phi_{S_{oxy}} \frac{\epsilon [CO_{ribo}] th}{\epsilon [CO_{ribo}] (th + th_{riboTop}) + \alpha th} [Photon] (1 - e^{-k_{qRibo} \Delta t})}\right] - [RFH^*] \cdot \left[1 - \frac{1}{1 + k_{qRadical} \cdot \Delta t \cdot [RFH^*]}\right]$$

(eq. 8)

where Φ_{ISC} is the quantum yield of intersystem crossing for riboflavin and $k_{qRadical}$ is the quenching rate of the riboflavin radical.

The concentration of the reduced form of riboflavin $[RFH_2]$ can be calculated by:

$$[RFH_2] = [RFH_2]_0 + [RFH^*] \cdot \left[1 - \frac{1}{1 + 2 \cdot k_{qRadical} \cdot \Delta t \cdot [RFH^*]}\right] - [RFH_2] \cdot \left[1 - e^{-\frac{k_{qRibo}}{k_{RFH_{ox}}}[CO_{oxy}] \cdot (1 - e^{-k_{RFH_{ox}} \Delta t})}\right]$$

(eq. 9)

and the resulting formation of hydrogen peroxide H_2O_2 is given by:

$$[H_2O_2] = [H_2O_2]_0 + [RFH_2] \cdot \left[1 - e^{-\frac{k_{qRibo}}{k_{RFH_{ox}}}[CO_{oxy}] \cdot (1 - e^{-k_{RFH_{ox}} \Delta t})}\right]$$

(eq. 10)

Finally, the formation of cross-links is determined by:

$$[CXL] = [CXL]_0 + [S_{oxy}] \cdot \left[1 - e^{-\frac{k_{RFH_{ox}}}{k_{EMox}}[EM] \cdot (1 - e^{-k_{EMox} \Delta t})}\right] \quad (\text{eq. 11})$$

where $[CXL]$ is the potential concentration of newly formed cross-links in the corneal stroma or at least proportional to it.

EXPERIMENTS

Two different sets of experiments were performed to analyze the efficacy of pulsed CXL and to study the effect of continuous-irradiation (standard) CXL in different species.

PULSED CXL

Sixty freshly enucleated porcine eyes were obtained from a local slaughterhouse and divided into five groups. All corneas were deepithelialized with a hockey-knife and 0.1% riboflavin solution was administered by applying a drop every 3 minutes for a total of 30 minutes. Several CXL protocols were applied to study the reaction mechanism in more detail.

The first group received 3 mW/cm² UV-A irradiation at 365 nm during 30 minutes (5.4 J/cm²), the second group received 9 mW/cm² during 10 min (5.4 J/cm²), the third group received 30 mW/cm² in 1s-on-1s-off pulses during 8 minutes (7.2 J/cm²), the fourth group received 100 mW/cm² in 1/10s-on-9/10s-off pulses during 9 minutes (5.4 J/cm²), and the fifth group received 100 mW/cm² in 1/100s-on-99/100s-off pulses during 9 minutes (0.54 J/cm²). The sixth group was not irradiated and served as control. The first three groups represent clinically applied CXL protocols. The fourth and fifth groups were designed to have an optimized on/off-ratio of UV irradiation (fast oxygen depletion versus slow oxygen replenishment²⁰) at standard fluence or at 1/10 of the standard fluence, respectively. An irradiance of 100 mW/cm² was chosen because it decreased the on/off ratio by factor 10 and at the same time maintained a fluence of 5.4 J/cm² and a similar overall UV irradiation time.

The corneas were excised with a scleral rim and full-thickness corneal flaps were obtained immediately after treatment. For this purpose, a customized blade holder was used to cut two 5-mm-width flaps from the central cornea in superior-inferior direction. Each flap was subsequently mounted in a stress-strain extensometer (iZwicki line; Zwick Roell, Ulm, Germany) with 4-mm effective length and subjected to two steps of uniaxial (1D) biomechanical testing: two cycles of preconditioning between 0.2 and 2 N and stress-relaxation at 2 N (corresponding to 580 kPa). 1D testing was chosen due to its simplicity and suitability to determine differences between CXL treatment conditions. Yet, compared to the natural stress situation of the cornea subjected to the intraocular pressure, 1D testing applies a more distinct stress distribution than biaxial tensile testing.³²

CONTINUOUS IRRADIATION (STANDARD) CXL IN DIFFERENT SPECIES

Rabbit eyes (New Zealand white rabbits, male, aged approximately 8 weeks, n = 2) were obtained immediately after termination of a prior experiment, which was not related to the eye. Six porcine eyes were obtained from a local slaughterhouse and used within 4 hours. The eyes were treated according to the standard Dres-

den protocol,¹ including deepithelialization, riboflavin soaking for 30 minutes, and irradiation with UV-A at 365 nm for 30 minutes. After treatment, corneal buttons were excised and mounted into a custom-made holder for 2D extensometry, fixing the corneas circumferentially at a diameter of 1 cm. The holder was placed in a stress-strain extensometer (iZwicki line; Zwick Roell) that was operated in indentation mode to apply tensile stress on the cornea. The testing procedure was similar to the one described above, with the difference of a greater 2D testing force (12.6 N for porcine, 6.3 N for lapine) to induce a similar stress of approximately 600 kPa. We used a 2D biomechanical analysis in this part of the study to have better comparability to our previously published stress relaxation curves³³ in murine corneas treated at different CXL conditions. The holder for murine corneas in those experiments had a diameter of 1.6 mm and the applied force to induce a stress of approximately 600 kPa was 0.4 N.

DATA ANALYSIS

The testXpert II (Zwick Roell) and Excel (Excel for Mac Version 14.5.4; Microsoft Corporation, Redmond, WA) software were used for data analysis. Statistical analysis was performed in SPSS software (version 23; SPSS, Inc., Chicago, IL). The data were tested for homogeneity of variance with the Levene method. Then one-way analysis of variance was applied to compare the remaining stress after 119 sec of stress-relaxation. The significance level was set to 5%.

CORRELATION OF THEORETICAL AND EXPERIMENTAL DATA

The comparison of the theoretical and the experimental parts of the study was performed in three steps for all experimental conditions: (1) calculation of the theoretically predicted concentrations of newly formed cross-links and (2) analysis of the obtained experimental stress relaxation data. To account for differences in corneal thickness between species, we applied the same stress (0.6 MPa) to every cornea. Differences in corneal diameter did not play a role, because strain is measured in percent. Also, for better comparability of the remaining stress after relaxation between 1D and 2D tests, the stiffening factor was calculated and used for further interpretation. (3) Correlation of (1) and (2).

RESULTS

RESULTS FROM THEORETICAL MODELING

Our model was used to predict fundamental characteristics of the CXL treatment that have been described previously, such as the penetration depth and oxygen depletion during UV irradiation.

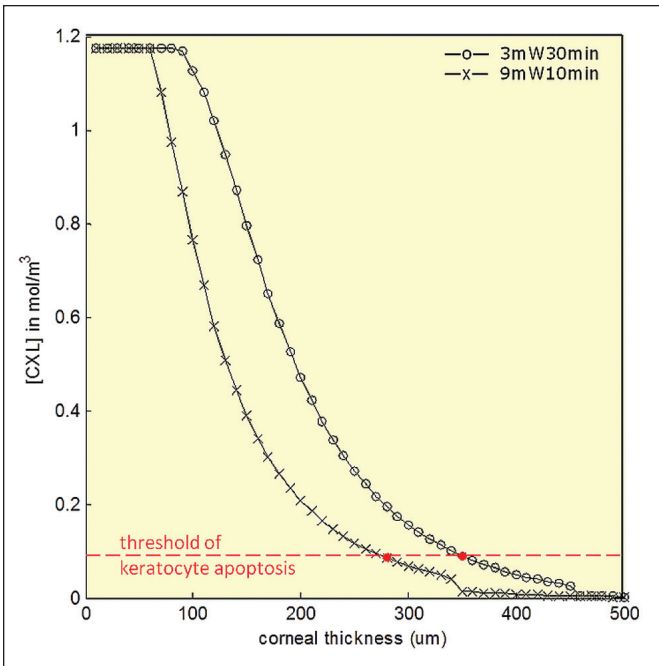


Figure 1. Theoretical prediction of the depth of effective corneal collagen cross-linking (CXL) (demarcation line). A more profound CXL was predicted with standard CXL compared to accelerated CXL, confirming clinical evidence.

DEMARICATION LINE

Figure 1 displays the theoretical prediction of the distribution of newly formed cross-links as a function of stromal depth. We could determine the theoretical threshold for effective CXL out from **Figure 1** by drawing a horizontal line that cuts the 3mW30min condition at 350 μm. The resulting demarcation line for 9mW10min as predicted from the model is then at 280 μm. Clinical studies have shown that standard CXL (3mW30min) induces a demarcation line at approximately 350.78 ± 49.34 μm depth, whereas accelerated CXL (9mW10min) induces a shallower demarcation line (288.46 ± 42.37 μm).²³

OXYGEN DEPLETION BELOW A 130-μM CORNEAL FLAP

A low-frequency pulsed UV irradiation (19min-on-9min-off, 3mW/cm²) was simulated, similar to the experiments presented in a recent study.²⁰ The prediction by our model matched the temporal course of the effective oxygen depletion under the 130-μm corneal flap (**Figure 2**).

EXPERIMENTAL RESULTS

Pulsed CXL. Measurements in porcine corneas following different pulsed and standard CXL protocols showed a significantly reduced stiffening effect at UV irradiation times shorter than 30 minutes, independent from the mode of UV administration. Standard CXL (442 ± 20 kPa)

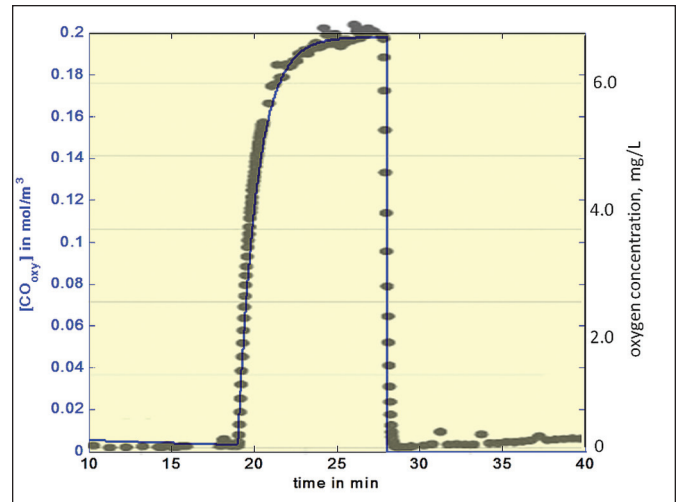


Figure 2. Oxygen depletion under a 130-μm flap as predicted from the model (blue line) and compared to previously published experimental data (black dots).²⁰

showed the strongest increase in stress resistance after relaxation (factor 1.21), compared to riboflavin control (365 ± 19 kPa). Continuous irradiation at 9 mW/cm² during 10 min (398 ± 26 kPa), pulsed irradiation at 30 mW/cm² with 1s-on-1s-off during 8 min (398 ± 33 kPa), and pulsed irradiation at 100 mW/cm² with 1/10s-on-9/10s-off during 9 min (393 ± 25 kPa) had a similar efficacy (**Figure 3**).

Statistical analysis revealed significant differences between standard CXL and riboflavin control ($P < .001$), between riboflavin and 9mW-10min_{cw} ($P = .005$), 30mW8min_{1s-on-1s-off} ($P = .017$), 100mW9min_{1/10s-on-9/10s-off} ($P = .004$), and 100mW9min_{1/100s-on-99/100s-off} ($P = .012$), and between standard CXL and 9mW10min_{cw} ($P = .002$), 30mW-8min_{1s-on-1s-off} ($P = .006$), 100mW_{9min1/10s-on-9/10s-off} ($P = .006$), and 100mW_{9min1/100s-on-99/100s-off} ($P = .001$). No differences ($P \geq .732$) were found between the conditions 9mW10min_{cw}, 30mW8min_{1s-on-1s-off}, 100mW_{9min1/10s-on-9/10s-off}, and 100mW_{9min1/100s-on-99/100s-off}. The condition 100mW/9min_{1/100s-on-99/100s-off} had a lower fluence, but induced the same mechanical stiffening as 9mW/10min_{cw} and the other pulsed CXL conditions.

Standard CXL in Different Species. Measurements of standard CXL in murine, lapine, and porcine corneas showed a clear linear relationship between CXL efficacy and corneal thickness (**Figure 4**). On average, the stiffening effect after CXL decreased by 4.1% per 100 μm. The R² value of the linear regression was 0.9961.

CORRELATION OF THEORETICAL AND EXPERIMENTAL DATA

Theoretical Concentration of Cross-links Versus Experimentally Obtained Stiffening Factor. **Figure 5** presents the scatter plot for the theoretical increase in

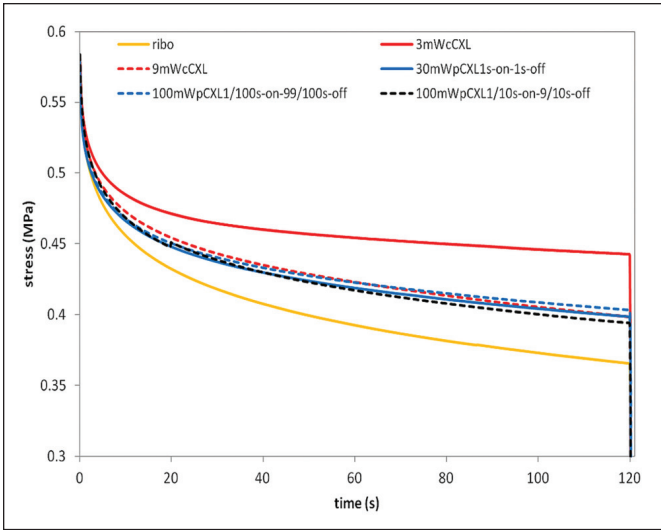


Figure 3. Stress-relaxation curves for the different conditions. The effect of corneal collagen cross-linking (CXL) is more dependent on the duration of the ultraviolet (UV) irradiation than to the overall applied UV fluence.

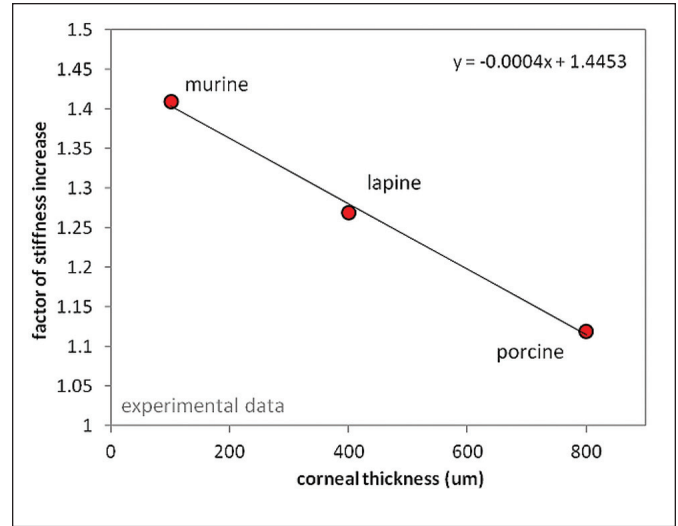


Figure 4. Experimental data show a linear decrease in the effect of the standard corneal collagen cross-linking (CXL) treatment with corneal thickness in different species. The stiffness increase was determined from 2D stress relaxation tests.

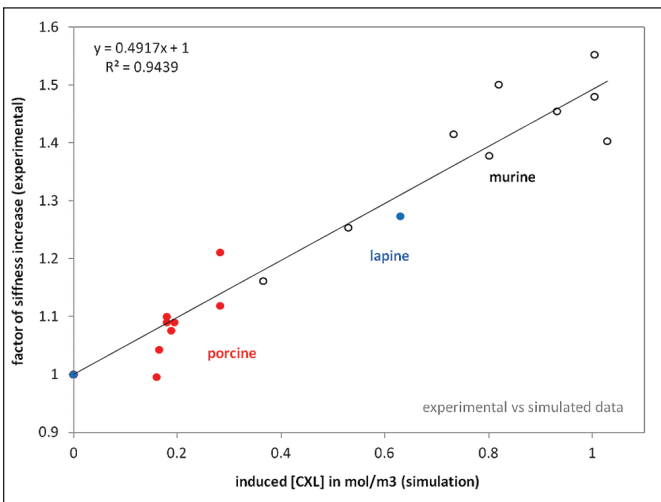


Figure 5. The scatter plot comparing the experimental stiffness increase with the predicted concentration of induced cross-links from simulation demonstrates a linear relationship. The stiffness increase was determined from 1D and 2D stress relaxation tests. CXL = corneal collagen cross-linking

concentration of cross-links and the corresponding experimentally obtained stiffening factor for all conditions that were analyzed in this study. We observed a clear linear relationship between both parameters with an R^2 value of 0.9432. Accordingly, an additional 1 mol/m³ of cross-links increases the mechanical stress resistance of the cornea by 50.4%.

Efficacy of Different CXL Protocols. Figure 6 shows the theoretical concentration of cross-links as a function of time. The number of cross-links reached at the end of the treatment is a measure of the increase of corneal stress resistance. Similarly, in Figure 1 the stress remaining after a relaxation period of 120 sec is a measure

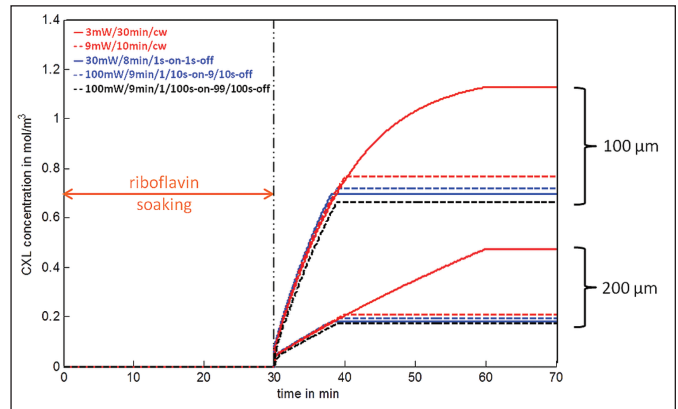


Figure 6. Corneal collagen cross-linking (CXL) concentration as a function of time according to the theoretical model at stromal depths of 100 and 200 μm : comparison between standard, accelerated, and pulsed CXL protocols.

for the experimental stress resistance. The comparison between Figure 1 and Figure 6 shows that experimentally and theoretically CXL efficacy match: standard CXL demonstrated a clear higher efficacy than accelerated CXL, whereas any of the pulsed CXL conditions showed an efficacy similar to accelerated CXL.

DISCUSSION

We present a theoretical model and algorithm to predict the biomechanical effect of CXL. The model considers UV fluence, riboflavin concentration, and irradiation time, but also oxygen availability and consumption during CXL. We provide experimental data to confirm the model's accuracy regarding different CXL protocols and different corneal thicknesses. A comparison to previously published data confirms

that the model can be used to predict the demarcation line and also reproduces well the oxygen consumption during UV irradiation below a 130- μm corneal flap.

Both experimental and theoretical data matched in the extent of corneal stiffening after CXL. We found that pulsed UV irradiation does not increase the biomechanical effect of CXL. Also, all accelerated and pulsed protocols were inferior to standard CXL (Dresden protocol). However, CXL protocols with irradiation times from 8 to 10 minutes had the same effect, independently of the mode of UV administration (pulsed and standard) (**Figure 3** and **Figure 6**). These observations suggest that the limiting factor in CXL is time rather than UV irradiance or fluence. The time factor is critically dependent on the oxygen diffusion rate and other reaction kinetics, which (under standard laboratory conditions [1,013 hPa, 21% O_2 , 25°C]) cannot be modified. **Figure 6** visualizes this context for two stromal depths demonstrating that the slope and hence the speed of cross-link formation is constant for the tested parameter variation.

We have assumed a factor of 400 in equation 5, which decreases the number of possible cross-links the more cross-links have been induced. If this factor, which represents the depletion of potential binding sites, is too small, the cross-linking density in the most anterior layer would be exceedingly high. As a consequence, the theoretical number of cross-links would not correlate linearly with the experimentally measured stiffening effect.

For the clinical setting, our results suggest that the UV intensity in the standard treatment might be reduced without losing the desired biomechanical effect. However, although at 10 minutes a 10 \times reduction of the UV fluence theoretically leads to 96.8% of the biomechanical stiffening (for a 500- μm cornea), at 30 minutes the same reduction in UV fluence leads to 89.5% of the stiffening. Further investigations are therefore needed to determine to which extent the fluence may be reduced at the same clinical success.

A reduction of the UV fluence would also allow us to perform CXL in corneas thinner than the current limit of 400 μm because the threshold for endothelial toxicity would not be surpassed. According to the Lambert–Beer law, for a treatment with 0.3mW/30min the corneal thickness could be as low as 88 μm , with 0.9mW/30min approximately 278 μm . However, the minimally required thickness for CXL at low irradiances may no longer be determined by the UV energy absorbed by the endothelium, but potentially by the penetration depth of singlet oxygen and therefore might require a higher riboflavin concentration.

A limitation of this work is the rough approximation of Fick's law, which leads to a slight overestima-

tion of the diffusion rates for long diffusion times. For the riboflavin diffusion, we tested a second approximation that slightly underestimates the diffusion rate. This induced a less than 1% variation in the stiffening effect, demonstrating that equation 1 is realistic in this context. Also, regarding the oxygen diffusion, we have verified that our model makes correct predictions regarding oxygen consumption and replenishment within the range of interest (**Figure 4**). Another limitation of this study is that many experimental parameters from the literature were used (**Table A**), potentially leading to an accumulated error.

In its current state, the proposed theoretical model can be used to predict the treatment effect of different CXL protocols and help in the safety evaluation in thin corneas. In the future, the model might be combined with mechanical models (numerical³⁴ or finite-element³⁵⁻³⁷) to determine the optimal irradiation protocol in a patient-specific manner. The findings of this study suggest that a longer irradiation should be performed at the steepest position of the cornea and a shorter irradiation in its periphery to obtain the maximal flattening effect, analog to the piXL technique³⁸ but with the difference that long irradiation is applied instead of high fluence. Another direct application of our findings could be the use of the iontophoresis approach³⁹ in combination with long irradiation for transepithelial CXL. Transepithelial CXL is comparable to standard CXL at a deeper stromal layer: the epithelium absorbs UV light and riboflavin similar to the stroma, but with the difference that the epithelium does not get stiffened. A longer irradiation would permit more oxygen to diffuse into the stroma and increase the amount of cross-links that can be generated.

To our knowledge, this is the first study that presents a theoretical model for CXL and directly compares its predictions to the actual experimental efficacy of a set of different CXL protocols. The advantage of our model is that it already can be applied for clinical studies. Among others, it predicts that CXL can even be performed in corneas thinner than the current limit of 400 μm , without the need of hypo-osmolar riboflavin or other supplements (contact lenses and stromal flaps), while still respecting safety restrictions. Clinical trials will be the next step.

CXL efficacy may be predicted by a combination of reaction kinetics and oxygen availability. Although the penetration depth is mainly determined by oxygen availability, the speed of cross-link formation depends on general reaction kinetics, oxygen availability, and, to a minor extent, UV intensity. Increasing CXL efficacy would require prolonged UV irradiation at reduced irradiances, or a higher oxygen pressure in the envi-

ronment. Pulsed CXL does not allow to accelerate CXL or to increase its efficacy when compared to standard CXL of the same irradiation time.

AUTHOR CONTRIBUTIONS

Study concept and design (SK); data collection (SK); analysis and interpretation of data (SK, FH); writing the manuscript (SK); critical revision of the manuscript (SK, FH); statistical expertise (SK); administrative, technical, or material support (FH); supervision (FH)

REFERENCES

- Wollensak G, Spörl E, Seiler T. Treatment of keratoconus by collagen cross linking [article in German]. *Ophthalmologe*. 2003;100:44-49.
- Koller T, Mrochen M, Seiler T. Complication and failure rates after corneal crosslinking. *J Cataract Refract Surg*. 2009;35:1358-1362.
- Mrochen M. Current status of accelerated corneal cross-linking. *Indian J Ophthalmol*. 2013;61:428-429.
- Leccisotti A, Islam T. Transepithelial corneal collagen cross-linking in keratoconus. *J Refract Surg*. 2010;26:942-948.
- Mastropasqua L, Nubile M, Calienno R, et al. Corneal cross-linking: intrastromal riboflavin concentration in iontophoresis-assisted imbibition versus traditional and transepithelial techniques. *Am J Ophthalmol*. 2014;157:623-630.
- Mazzotta C, Traversi C, Caragiuli S, Rechichi M. Pulsed vs continuous light accelerated corneal collagen crosslinking: in vivo qualitative investigation by confocal microscopy and corneal OCT. *Eye (Lond)*. 2014;28:1179-1183.
- Touboul D, Efron N, Smadja D, Praud D, Malet F, Colin J. Corneal confocal microscopy following conventional, transepithelial, and accelerated corneal collagen cross-linking procedures for keratoconus. *J Refract Surg*. 2012;28:769-775.
- Tomita M, Mita M, Huseynova T. Accelerated versus conventional corneal collagen crosslinking. *J Cataract Refract Surg*. 2014;40:1013-1020.
- Hammer A, Richoz O, Mosquera SA, Tabibian D, Hoogewoud F, Hafezi F. Corneal biomechanical properties at different corneal cross-linking (CXL) irradiances corneal biomechanics at higher UV-A Irradiances. *Invest Ophthalmol Vis Sci*. 2014;55:2881-2884.
- Kanellopoulos AJ, Loukas YL, Asimellis G. Cross-linking biomechanical effect in human corneas by same energy, different UV-A fluence: an enzymatic digestion comparative evaluation. *Cornea*. 2016;35:557-561.
- Schumacher S, Oeftiger L, Mrochen M. Equivalence of biomechanical changes induced by rapid and standard corneal cross-linking, using riboflavin and ultraviolet radiation. *Invest Ophthalmol Vis Sci*. 2011;52:9048-9052.
- Aldahlawi NH, Hayes S, O'Brart DP, Meek KM. Standard versus accelerated riboflavin-ultraviolet corneal collagen crosslinking: resistance against enzymatic digestion. *J Cataract Refract Surg*. 2015;41:1989-1996.
- Kling S, Remon L, Pérez-Escudero A, Merayo-Llodes J, Marcos S. Corneal biomechanical changes after collagen cross-linking from porcine eye inflation experiments. *Invest Ophthalmol Vis Sci*. 2010;51:3961-3968.
- Kling S, Richoz O, Hammer A, et al. Increased biomechanical efficacy of corneal cross-linking in thin corneas due to higher oxygen availability. *J Refract Surg*. 2015;31:840-846.
- Scarcelli G, Kling S, Quijano E, Pineda R, Marcos S, Yun SH. Brillouin microscopy of collagen crosslinking: noncontact depth-dependent analysis of corneal elastic modulus Brillouin microscopy of collagen crosslinking. *Invest Ophthalmol Vis Sci*. 2013;54:1418-1425.
- Spoerl E, Wollensak G, Seiler T. Increased resistance of cross-linked cornea against enzymatic digestion. *Curr Eye Res*. 2004;29:35-40.
- Wollensak G, Spoerl E, Seiler T. Stress-strain measurements of human and porcine corneas after riboflavin-ultraviolet-A-induced cross-linking. *J Cataract Refract Surg*. 2003;29:1780-1785.
- Schumacher S, Mrochen M, Wernli J, Bueeler M, Seiler T. Optimization model for UV-riboflavin corneal cross-linking. *Invest Ophthalmol Vis Sci*. 2012;53:762-769.
- Semchishen A, Mrochen M, Semchishen V. Model for Optimization of the UV-A/riboflavin strengthening (cross-linking) of the cornea: percolation threshold. *Photochem Photobiol*. 2015;91:1403-1411.
- Kamaev P, Friedman MD, Sherr E, Muller D. Photochemical kinetics of corneal cross-linking with riboflavin. *Invest Ophthalmol Vis Sci*. 2012;53:2360-2367.
- Richoz O, Hammer A, Tabibian D, Gatzoufas Z, Hafezi F. The biomechanical effect of corneal collagen cross-linking (CXL) with riboflavin and UV-A is oxygen dependent. *Transl Vis Sci Technol*. 2013;2:6.
- Kanellopoulos AJ, Asimellis G. Introduction of quantitative and qualitative cornea optical coherence tomography findings induced by collagen cross-linking for keratoconus: a novel effect measurement benchmark. *Clin Ophthalmol*. 2013;7:329.
- Kymionis GD, Tsoulnaras KI, Grentzelos MA, et al. Corneal stroma demarcation line after standard and high-intensity collagen crosslinking determined with anterior segment optical coherence tomography. *J Cataract Refract Surg*. 2014;40:736-740.
- Seiler T, Hafezi F. Corneal cross-linking-induced stromal demarcation line. *Cornea*. 2006;25:1057-1059.
- Chacon JN, McLearie J, Sinclair RS. Singlet oxygen yields and radical contributions in the dye-sensitized photo-oxidation in methanol of esters of polyunsaturated fatty acids (oleic, linoleic, lonolenic and archidonic). *Photochem Photobiol*. 1988;47:647-656.
- Baier J, Maisch T, Maier M, Engel E, Landthaler M, Bäuml W. Singlet oxygen generation by UVA light exposure of endogenous photosensitizers. *Biophysical J*. 2006;91:1452-1459.
- Huang R, Choe E, Min DB. Kinetics for singlet oxygen formation by riboflavin photosensitization and the reaction between riboflavin and singlet oxygen. *J Food Sci*. 2004;69:C726-C732.
- Manso JA, Pérez-Prior MT, García-Santos MDP, Calle E, Casado J. A kinetic approach to the alkylating potential of carcinogenic lactones. *Chem Res Toxicol*. 2005;18:1161-1166.
- Freeman RD. Oxygen consumption by the component layers of the cornea. *J Physiol*. 1972;225:15-32.
- Fatt I, Freeman RD, Lin D. Oxygen tension distributions in the cornea: a re-examination. *Exp Eye Res*. 1974;18:357-365.
- Wollensak G, Aurich H, Wirbelauer C, Sel S. Significance of the riboflavin film in corneal collagen crosslinking. *J Cataract Refract Surg*. 2010;36:114-120.
- Kanellopoulos AJ, Asimellis G, Salvador-Culla B, Chodosh J, Ciolino JB. High-irradiance CXL combined with myopic LASIK: flap and residual stroma biomechanical properties studied ex-vivo. *Br J Ophthalmol*. 2015;99:870-874.

33. Hammer A, Kling S, Boldi M-O, et al. Establishing corneal cross-linking with riboflavin and UV-A in the mouse cornea in vivo: biomechanical analysis corneal cross-linking in mice. *Invest Ophthalmol Vis Sci.* 2015;56:6581-6590.
34. Pandolfi A, Manganiello F. A model for the human cornea: constitutive formulation and numerical analysis. *Biomech Model Mechanobiol.* 2006;5:237-246.
35. Dupps WJ Jr. Biomechanical modeling of corneal ectasia. *J Refract Surg.* 2005;21:186-190.
36. Kling S, Bekesi N, Dorronsoro C, Pascual D, Marcos S. Corneal viscoelastic properties from finite-element analysis of in vivo air-puff deformation. *PLoS One.* 2014;9:e104904.
37. Pinsky PM, Datye DV. A microstructurally-based finite element model of the incised human cornea. *J Biomechanics.* 1991;24:907-922.
38. Kanellopoulos AJ, Asimellis G. Presbyopic PiXL cross-linking. *Curr Ophthalmol Rep.* 2015;3:1-8.
39. Mastropasqua L, Nubile M, Calienno R, et al. Corneal cross-linking: intrastromal riboflavin concentration in iontophoresis-assisted imbibition versus traditional and transepithelial techniques. *Am J Ophthalmol.* 2014;157:623-630.
40. Au V, Madison SA. Effects of singlet oxygen on the extracellular matrix protein collagen: oxidation of the collagen crosslink histidinohydroxylysionorleucine and histidine. *Arch Biochem Biophys.* 2000;384:133-142.
41. Koppen C, Gobin L, Tassignon MJ. The absorption characteristics of the human cornea in ultraviolet-a crosslinking. *Eye Contact Lens.* 2010;36:77-80.
42. Larrea X, Büchler P. A transient diffusion model of the cornea for the assessment of oxygen diffusivity and consumption. *Invest Ophthalmol Vis Sci.* 2009;50:1076-1080.
43. Ahmad I, Fasihullah Q, Noor A, Ansari IA, Ali QNM. Photolysis of riboflavin in aqueous solution: a kinetic study. *Int J Pharmaceutics.* 2004;280:199-208.
44. Matheson IBC, Etheridge RD, Kratowich NR, Lee J. The quenching of singlet oxygen by amino acids and proteins. *Photochem Photobiol.* 1975;21:165-171.

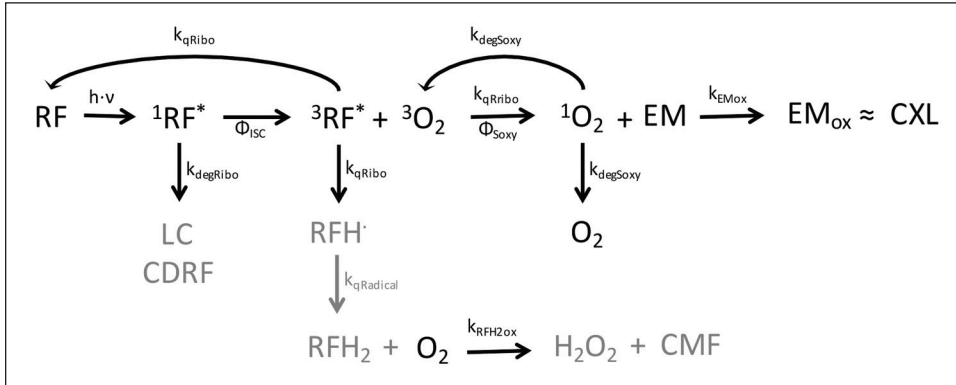


Figure A. Chemical reaction scheme for the formation of additional cross-links in the corneal stroma during corneal collagen cross-linking (CXL). RF = riboflavin; 1RF* = excited singlet state of riboflavin; 3RF* = excited triplet state of riboflavin; 3O₂ = excited triplet state of oxygen; 1O₂ = excited singlet state of oxygen; O₂ = molecular oxygen; EM = extracellular matrix; CXL = additional cross-links; LC = lumichrome; CDRF = cyclodehydroriboflavin; RFH· = riboflavin radical; RFH₂ = reduced form of riboflavin; H₂O₂ = hydrogen peroxide; CMF = carbomethylflavin

TABLE A
Parameters and Values as Used in the Theoretical Model

Parameter	Value	Description	Literature
Φ_{ISC}	0.61	Quantum yield of intersystem crossing for riboflavin	Chacon et al. ²⁵
Φ_{Soxy}	0.54	Quantum yield of singlet oxygen production for riboflavin	Baier et al. ²⁶
α	267 m ⁻¹	Absorption coefficient of the corneal stroma	Kamaev et al. ²⁰
ϵ	1,339.3 m ³ ·(mol·m) ⁻¹	Extinction coefficient of riboflavin	The authors' fit to data taken from Koppen et al. ⁴¹
Δ_{ribo}	4·10 ⁻¹¹ m ² ·s ⁻¹	Diffusion coefficient of riboflavin into the cornea	Kamaev et al. ²⁰
Δ_{oxy}	8·10 ⁻¹⁰ m ² ·s ⁻¹	Diffusion coefficient of oxygen into the cornea	Similar to the range previously reported ^{20,42}
Q_{cell}	1.4·10 ⁻⁵ ml _{O₂} ·(ml _{tissue} ·s) ⁻¹	Stromal oxygen consumption at an oxygen tension of 160 mm Hg; a linear relation between oxygen consumption and tension was considered in the model	Freeman ²⁹
$k_{degRibo}$	7.08·10 ⁻⁵ s ⁻¹	Rate constant of riboflavin degeneration due to photolysis	Ahmad et al. ⁴³
$k_{degSoxy}$	2.56·10 ⁵ s ⁻¹	Rate constant of singlet oxygen degeneration due to quenching	Huang et al. ²⁷
k_{qRibo}	3.2·10 ⁶ s ⁻¹	Rate constant of riboflavin triplet quenching to produce singlet oxygen	Baier et al. ²⁶
$k_{qRadical}$	3·10 ⁵ s ⁻¹	Rate constant of riboflavin radical quenching to produce reduced riboflavin	Kamaev et al. ²⁰
k_{EMox}	1.7·10 ⁵ s ⁻¹	Rate constant of extracellular matrix oxidation by singlet oxygen (chemical quenching by histidine)	Matheson et al. ⁴⁴
K_{RFH2ox}	150 s ⁻¹	Rate constant of reduced riboflavin oxidation by oxygen	The authors' estimate